

SiReN: Sign-Aware Recommendation Using Graph Neural Networks

Changwon Seo, Kyeong-Joong Jeong, Sungsu Lim, *Member, IEEE*, and Won-Yong Shin, *Senior Member, IEEE*

Abstract—In recent years, many recommender systems using network embedding (NE) such as graph neural networks (GNNs) have been extensively studied in the sense of improving recommendation accuracy. However, such attempts have focused mostly on utilizing only the information of positive user–item interactions with high ratings. Thus, there is a challenge on how to make use of *low rating* scores for representing users’ preferences since low ratings can be still informative in designing NE-based recommender systems. In this study, we present **SiReN**, a new *Sign-aware Recommender* system based on GNN models. Specifically, **SiReN** has three key components: 1) constructing a *signed* bipartite graph for more precisely representing users’ preferences, which is split into two edge-disjoint graphs with *positive* and *negative* edges each, 2) generating two embeddings for the partitioned graphs with positive and negative edges via a GNN model and a multi-layer perceptron (MLP), respectively, and then using an attention model to obtain the final embeddings, and 3) establishing a sign-aware Bayesian personalized ranking (BPR) loss function in the process of optimization. Through comprehensive experiments, we empirically demonstrate that **SiReN** consistently outperforms state-of-the-art NE-aided recommendation methods.

Index Terms—Bayesian personalized ranking (BPR) loss, graph neural network, network embedding, recommender system, signed bipartite graph.

I. INTRODUCTION

A. Background and Motivation

RECOMMENDER systems have been widely advocated as a way of providing suitable recommendation solutions to customers in various fields such as e-commerce, advertising, and social media sites. One of the most important and popular techniques in recommender systems is collaborative filtering (CF), which computes similarities between users and items from historical interactions (e.g., clicks and purchases) to suggest relevant items to users by assuming that users who have behaved similarly with each other exhibit similar preferences for items [1]–[3]. Moreover, following up the great success of network embedding (NE), also known as network representation learning, considerable research attention has been paid to NE-based recommender systems that attempt to model high-order connectivity information from user–item interactions viewed as a bipartite graph [4]–[7].¹ In recent years,

C. Seo, K.-J. Jeong, and W.-Y. Shin are with the School of Mathematics and Computing (Computational Science and Engineering), Yonsei University, Seoul 03722, Republic of Korea (e-mail: {changwoni, jeongkj, wy.shin}@yonsei.ac.kr).

S. Lim is with the Department of Computer Science and Engineering, Chungnam National University, Daejeon 34134, Republic of Korea (e-mail: sungsu@cnu.ac.kr).

(Corresponding author: Won-Yong Shin.)

¹In the following, we use the terms “graph” and “network” interchangeably.

graph neural networks (GNNs) [8]–[12] have emerged as a powerful neural architecture to learn vector representations of nodes and graphs. By virtue of great prowess in solving various downstream machine learning problems, GNN-based recommender systems [13]–[19] have also been developed for improving the recommendation accuracy.

GNN models are basically trained by aggregating the information of direct neighbor nodes via message passing under the *homophily* (or *assortativity*) assumption that a target node and its neighbors are similar to each other [12]. Due to the neighborhood aggregation mechanism, existing literature posits that high homophily of the underlying graph is a necessity for GNNs to achieve good performance especially on node classification [20]–[22]. On the other hand, in recommender systems, while users’ feedback on many online websites (e.g., *likes/dislikes* on YouTube and high/low ratings on Amazon) can be positive and negative, existing GNN-based recommender systems overlook the existence of negative feedback (i.e., user–item interactions with low ratings) due to their ease of modeling. Precisely, most GNN-based approaches utilize only positive feedback by removing the negative interactions in order to exhibit strong homophily in neighbors (see Fig. 1).² It is worthwhile to note that, despite the remarkable performance boost by existing GNN-based recommender systems, the low ratings can be still informative. This is because such information expresses signs of what users *dislike*. In other words, full exploitation of two types of feedback in GNNs may have the potential to further improve the recommendation performance, which remains a new design challenge.

B. Main Contributions

Even with the wide applications of GNNs to recommender systems [13]–[19], a question that arises naturally is: “How can we make use of negative feedback (i.e., low rating scores) for representing users’ preferences via GNNs?”. In this paper, to answer this question, we introduce **SiReN**, a *Sign-aware Recommender* system based on GNN models. To this end, we design and optimize our new GNN-aided learning model while distinguishing users’ positive and negative feedback.

Our proposed **SiReN** method includes three key components: 1) signed graph construction and partitioning, 2) model architecture design, and 3) model optimization. First,

²A graph is usually referred to as homophilous (or assortative) if connected nodes are much more likely to have the same class label than if edges are independent of labels. In our study, a *homophilous bipartite* graph assumes that user–item relations are significantly more likely to be positive.

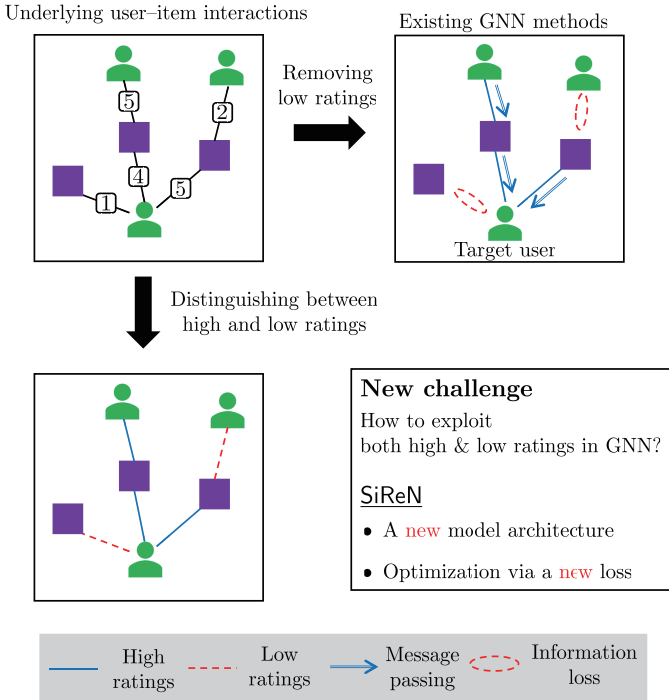


Fig. 1: New challenges in GNN-based recommender systems.

to overcome the primary problem of existing GNN-based recommender systems [15], [18], [19] that fail to learn both positive and negative relations between users and items, we start by constructing a *signed* bipartite graph, which is split into two edge-disjoint graphs with *positive* and *negative* edges each. This signed graph construction and partitioning process enables us to more distinctly identify users’ preferences for observed items. Second, we show how to design our model architecture for discovering embeddings of all users and items in the signed bipartite graph. Although several GNN models were introduced in [23], [24] for signed unipartite graphs, simply applying them to recommender systems, corresponding to user-item bipartite graphs, may not be desirable. This is because such GNN models were built upon the assumption of balance theory [25], which implies that “*the friend of my friend is my friend*” and “*the enemy of my enemy is my friend*”. However, the balance theory no longer holds in recommender systems since users’ preferences cannot be dichotomous. In other words, users are likely to have dissimilar preferences even if they dislike the same item(s). This motivates us to design our own model architecture for each partitioned graph, rather than employing existing GNN approaches based on the balance theory. Concretely, SiReN contains three learning models. For the graph with positive edges, we employ a GNN model suit for recommender systems. For the graph with negative edges, we adopt a multi-layer perceptron (MLP) due to the fact that negative edges can weaken the homophily and thus message passing to such dissimilar nodes would not be feasible. To obtain the final embeddings, we then use an attention model that learns the importance of two embeddings generated from GNN and MLP models. Third, as our objective function in the process of optimization, we

present a *sign-aware* Bayesian personalized ranking (BPR) loss function, which is built upon the original BPR loss [26] widely used in recommender systems. More specifically, unlike the original BPR loss, our objective function takes into account two types of observed items, including both positive and negative relations between users and items, as well as unobserved ones.

To validate the superiority of our SiReN method, we comprehensively perform empirical evaluations using various real-world datasets. Experimental results show that our method consistently outperforms state-of-the-art GNN methods for top- N recommendation in terms of several recommendation accuracy metrics. Such a gain is possible owing to the use of low rating information along with judicious model design and optimization. We also empirically validate the effectiveness of MLP in comparison with other model architectures used for the graph with negative edges. Additionally, our experimental results demonstrate the robustness of our SiReN method to more challenging interaction sparsity levels.

It is worth noting that our method is GNN-*model-agnostic* and thus any competitive GNN architectures can be appropriately chosen for potentially better performance. The main technical contributions of this paper are four-fold and summarized as follows:

- We propose SiReN, a novel GNN-aided recommender system that makes full use of the user-item interaction information after signed graph construction and partitioning;
- We design our model architecture using three learning models in the sense of utilizing sign awareness so as to generate embeddings of users and items;
- We establish the sign-aware BPR loss as our objective function;
- We validate SiReN through extensive experiments using three real-world datasets while showing the superiority of our method over state-of-the-art NE-aided methods under diverse conditions.

C. Organization and Notation

The remainder of this paper is organized as follows. In Section II, we present prior studies related to our work. In Section III, we explain the methodology of our study, including basic settings and an overview of our SiReN method. Section IV describes technical details of the proposed method. Comprehensive experimental results are shown in Section V. Finally, we provide a summary and concluding remarks in Section VI.

Table I summarizes the notation that is used in this paper. This notation will be formally defined in the following sections when we introduce our methodology and the technical details.

II. RELATED WORK

The method that we proposed in this study is related to two broader research lines, namely standard CF approaches and NE-based recommendation approaches.

Notation	Description
G	Given weighted bipartite graph
\mathcal{U}	Set of users in G
\mathcal{V}	Set of items in G
\mathcal{E}	Set of weighted edges in G
M	Number of users
N	Number of items
G^s	Signed bipartite graph constructed from G
\mathcal{E}^s	Set of signed edges in G^s
G^p	Partitioned graph with positive edges
\mathcal{E}^p	Set of positive edges in G^p
G^n	Partitioned graph with negative edges
\mathcal{E}^n	Set of negative edges in G^n
\mathbf{Z}^p	Embeddings for all nodes in G^p
\mathbf{Z}^n	Embeddings for all nodes in G^n
\mathbf{Z}	Final embeddings
α^p	Importance of \mathbf{Z}^p
α^n	Importance of \mathbf{Z}^n
θ_1	Model parameters of GNN
θ_2	Model parameters of MLP
θ_3	Model parameters of ATTENTION

TABLE I: Summary of notations.

A. Standard CF Approaches

As one of the most popular techniques, CF in recommender systems aims to capture the relationships between users and items from historical interactions (e.g., ratings and purchases) by discovering learnable vector representations for users and items based on a rating matrix [2], [27]. Matrix factorization (MF) [28] decomposes the user–item interaction matrix into a product of two low-dimensional matrices and models their similarities with the dot product of two matrices. ANLF [29] was designed based on a non-negative MF (NMF) model [30] using the alternating direction method. In DMF [31] and NCF [32], MF models with neural network architectures were proposed to project users and items into a latent structured space. Moreover, SLIM [33] proposed a sparse linear model by directly reconstructing the low-density user–item interaction matrix. To capture complex relationships between items in sparse datasets, FISM [34] and NPE [35] showed how to learn item–item similarities as the product of two latent factor matrices. While MF-based models such as [31], [32] rely on the dot product of user and item latent vectors as a similarity measure, CML [1] showed how to learn a joint metric space to encode not only users’ preferences but also user–user and item–item similarities in the Euclidean distance. In NAIS [36], the attention mechanism was incorporated to obtain the importance of each item from user–item interactions for preference prediction. DLMF [37] designed a trust-aware recommender system that leverages deep learning to determine the initialization in MF by synthesizing the users’ interests and their trusted friends’ interests in addition to the user–item interactions.

B. NE-Based Recommendation Approaches

Recently, it has been comprehensively studied how to develop recommender systems using NE. While standard CF approaches are capable of only modeling the first-order connectivity between users and items, NE-based approaches aim to exploit *high-order proximity* among users and items through the user–item bipartite graph structure [15], [19]. BiNE [6] and CSE [7] were developed based on random walks in order to infer similar users (or items) in the underlying bipartite graph (i.e., user–item interactions).

Moreover, encouraged by the success of GNNs in solving many graph mining tasks [12], GNN-based recommender systems have more recently emerged as promising techniques [13]–[19], [38], [39]. Existing GNN models for top- N recommendation were generally developed using implicit feedback, which treats observed user–item interactions as positive relations. GC-MC [38] presented a graph autoencoder including graph convolutions for rating matrix completion. PinSage [13] showed a scalable GNN framework developed in production at Pinterest by improving upon GraphSAGE [9] along with several aggregation functions. Spectral CF [14] presented a spectral convolution operation to learn the rich information of connectivity between users and items in the spectral domain. As state-of-the-art NE-based recommender systems using only user–item interactions as input, NGCF [15], LR-GCCF [18], and LightGCN [19] were developed based on GCN [8], the first attempt to apply convolutions to graph domains, while performing layer aggregation to solve the over-smoothing problem. IGMCC [39] proposed an inductive GNN-based matrix completion model that learns local subgraphs in the underlying user–item interaction matrix. To explore users’ latent purchasing motivations (e.g., cost effectiveness and appearance), MCCF [16] presented a CF approach based on GNNs for generating multiple user/item embeddings and then combining them via attention mechanisms. AGCN [17] proposed a GCN approach for joint item recommendation and attribute inference in an attributed user–item bipartite graph with incomplete attribute values.

To alleviate the sparsity of user–item interactions, each user’s local neighbors’ preferences in social networks were also utilized in [40]–[42] for better user embedding modeling, thus enabling us to improve the recommendation accuracy.

C. Discussions

Despite the aforementioned contributions, leveraging *explicit feedback* data (i.e., user–item interactions with ratings) in NE-based approaches has been largely underexplored in the literature. To learn vector representations for users and items based on the NE, it is common to utilize only positive user–item interactions as observed data when explicit feedback data are given (see [7], [40], [42] and references therein). However, negative interactions with low ratings can be still informative since such information shows signs of what users *dislike*. It remains open how to make use of low ratings in designing NE-aided recommender systems.

On the other hand, several GNN models were developed in [23], [24] to learn vector representations of nodes in *signed*

(unipartite) graphs with both positive and negative edges based on the structural balance theory [25]. However, it is worth noting that the balance theory does not hold in recommender systems due to the fact that users’ preferences cannot be dichotomous, i.e., a behavior of users disliking similar items does not always imply the same degree of user preferences about items. Therefore, adopting such GNN methods designed for signed graphs would not be desirable to capture different levels of user preferences.

III. METHODOLOGY

In this section, we describe our network model with basic settings. Next, we explain an overview of the proposed SiReN method as a solution to the problem of making full use of low ratings in GNN models.

A. Network Model and Basic Settings

In recommender systems, the basic input is the historical user–item interactions with ratings, which is represented as a weighted bipartite graph. Let us denote the underlying bipartite graph as $G = (\mathcal{U}, \mathcal{V}, \mathcal{E})$, where \mathcal{U} and \mathcal{V} are the set of M users and the set of N items, respectively, and \mathcal{E} is the set of weighted edges between \mathcal{U} and \mathcal{V} . A weighted edge $(u, v, w_{uv}) \in \mathcal{E}$ can be interpreted as the rating w_{uv} with which the user $u \in \mathcal{U}$ has given to the item $v \in \mathcal{V}$. We assume G to be a static network without repeated edges, where ratings (i.e., user preferences) do not change over time.

In our study, we aim at designing a new GNN-aided recommender system for improving the accuracy of top- N recommendation by making full use of the user–item rating information in G , including *low ratings* that have not been explored by conventional GNN-based recommender systems [18], [19], without any side information.

B. Overview of SiReN

In this subsection, we explain our methodology along with the overview of the proposed SiReN method. We recall that our study is motivated by the fact that recent recommender systems built upon GNN models such as [18], [19] take advantage of only high rating scores as observed data by deleting some edges, corresponding to low ratings (e.g., the rating scores of 1 and 2 in the 1–5 rating scale), in the set \mathcal{E} over the weighted bipartite graph G [7], [40], [42]. This is because such a removal of low ratings from G enables us to aggregate the positively connected neighbors via message passing in GNNs. However, the set of negative interactions indicates what users *dislike* and thus is still quite informative. In other words, it remains open how to fully exploit the rating information in building GNN-based recommender systems as recently developed models fail to capture the effect of low rating scores.

To tackle this challenge, we present SiReN, a new *sign-aware* recommender system using GNNs, which is basically composed of the following three core components (refer to Fig. 2):

- signed bipartite graph construction and partitioning

- embedding generation for each partitioned graph
- optimization via a sign-aware BPR loss.

First, we describe how to construct a signed bipartite graph G^s that enables us to more distinctly identify users’ preferences based on all the user–item interactions. More specifically, we construct $G^s = (\mathcal{U}, \mathcal{V}, \mathcal{E}^s)$ with a parameter $w_o > 0$, representing a criterion for dividing high and low ratings, where

$$\mathcal{E}^s = \{(u, v, w_{uv}^s) \mid w_{uv}^s = w_{uv} - w_o, (u, v, w_{uv}) \in \mathcal{E}\}. \quad (1)$$

Here, w_o can be determined according to characteristics (e.g., the rating scale and the popularity distribution of items) of a given dataset; from an algorithm design perspective, we assume that a user u likes an item v if $w_{uv}^s > 0$ and he/she dislikes v otherwise, where $w_{uv}^s = w_{uv} - w_o$ corresponds to the edge weight in the signed bipartite graph G^s . Note that, although representation learning, including GNNs, on signed graphs has been studied in [23], [24], [43], designing GNN-based recommender systems on signed bipartite graphs has never been conducted in the literature. Basically, GNN models are trained by aggregating the information of neighbor nodes under the *homophily* assumption [12]. However, due to the fact that the signed graph G^s includes negative edges (i.e., interactions with low ratings), aggregating the information of such negatively connected neighbors may not be desirable. As illustrated in Fig. 2, to more delicately capture each relation of positively and negatively connected neighbors, we then *partition* the signed bipartite graph G^s into two edge-disjoint graphs $G^p = (\mathcal{U}, \mathcal{V}, \mathcal{E}^p)$ and $G^n = (\mathcal{U}, \mathcal{V}, \mathcal{E}^n)$, consisting of the set of positive edges and negative edges, respectively. Here, it follows that $\mathcal{E}^s = \mathcal{E}^p \cup \mathcal{E}^n$, where

$$\mathcal{E}^p = \{(u, v, w_{uv}^s) \mid w_{uv}^s > 0, (u, v, w_{uv}^s) \in \mathcal{E}^s\} \quad (2a)$$

$$\mathcal{E}^n = \{(u, v, w_{uv}^s) \mid w_{uv}^s < 0, (u, v, w_{uv}^s) \in \mathcal{E}^s\}. \quad (2b)$$

The purpose of this graph partitioning is to make the graphs G^p and G^n , respectively, assortative and disassortative so that each partitioned graph is used as input to the most appropriate learning model.

Second, we describe how to generate embeddings of M users and N items along with three learning models in our SiReN method. Using the graph G^p having positive edges, we adopt a GNN model suit for recommender systems (e.g., [18], [19]) to calculate embedding vectors $\mathbf{Z}^p \in \mathbb{R}^{(M+N) \times d}$ for the nodes in $\mathcal{U} \cup \mathcal{V}$:

$$\mathbf{Z}^p = \text{GNN}_{\theta_1}(G^p), \quad (3)$$

where d is the dimension of the embedding space and θ_1 is the learned model parameters of GNN. On the other hand, we adopt an MLP for the graph G^n to calculate embedding vectors $\mathbf{Z}^n \in \mathbb{R}^{(M+N) \times d}$ for the same nodes as those in (3):

$$\mathbf{Z}^n = \text{MLP}_{\theta_2}(G^n), \quad (4)$$

where θ_2 is the learned model parameters of MLP. We would like to state the following two remarks to explain the model selection according to types of graphs.

Remark 1. *It is worth noting that existing GNN models, built upon message passing architectures, work on the basic*

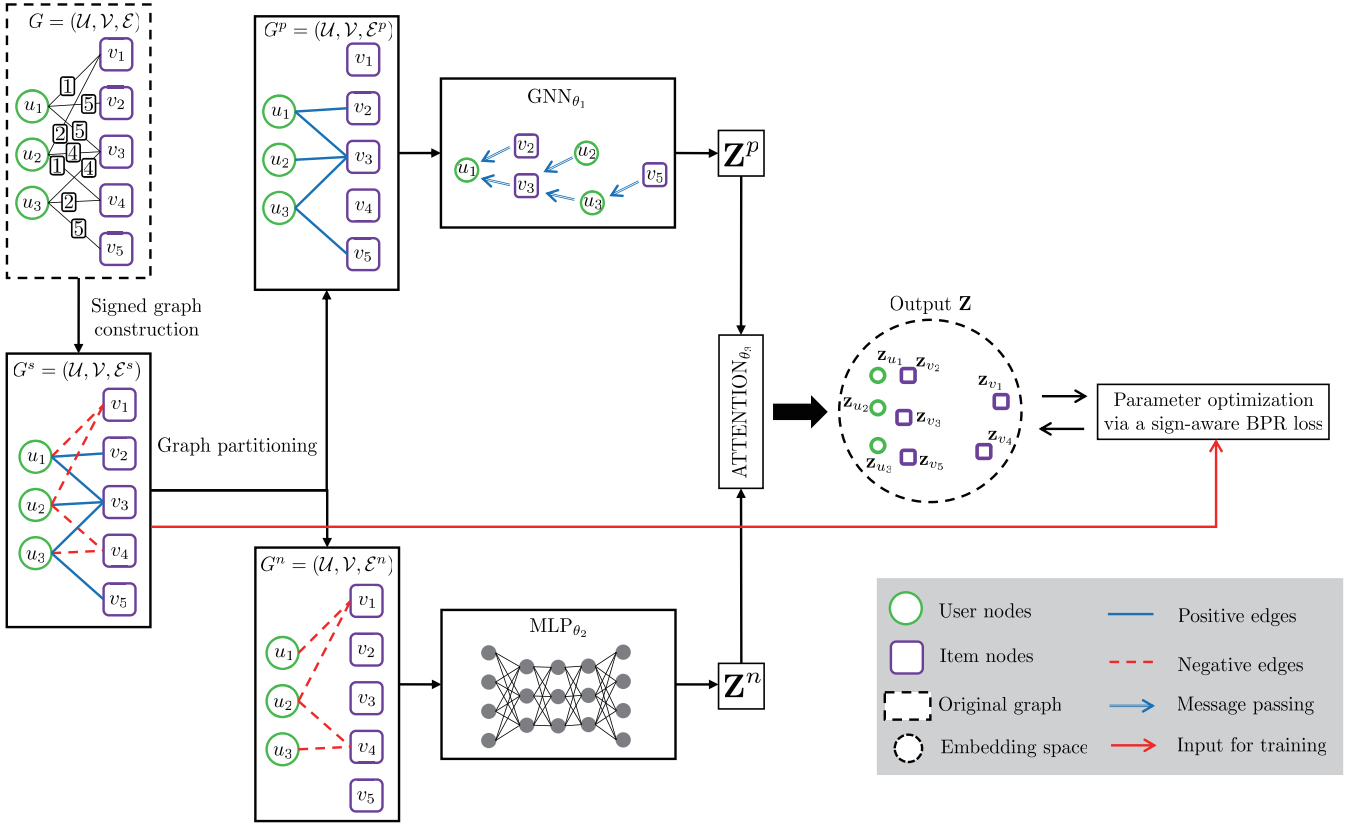


Fig. 2: The schematic overview of our SiReN method.

assumption of homophily [22]. We recall that users who dislike similar items may not have similar preferences (i.e., the tendency in rating items) with each other. Negative edges in G^n can undermine the effect of homophily and thus message passing to such dissimilar nodes would not be feasible. For these reasons, adopting GNNs in the graph with negative edges may not be desirable, based on the fact that many GNNs fail to generalize to disassortative graphs, i.e., graphs with low levels of homophily [20], [21], [44].

Remark 2. Additionally, note that the MLP architecture itself does not exploit the topological information. However, it does not imply that the connectivity information in the graph G^n is not used at all. In the optimization step, we update the embedding vectors in (3) and (4) by fully taking advantage of the set \mathcal{E}^n in G^n as well as the set \mathcal{E}^p in G^p , which will be specified later.

Next, let us mention another training model in SiReN, the so-called *attention* model. To get the importance of two embeddings \mathbf{Z}^p and \mathbf{Z}^n , we use the attention mechanism [45] that learns the corresponding importance (α^p, α^n) as follows:

$$(\alpha^p, \alpha^n) = \text{ATTENTION}_{\theta_3}(\mathbf{Z}^p, \mathbf{Z}^n), \quad (5)$$

which results in the final embeddings:

$$\mathbf{Z} = (\alpha^p \mathbf{1}_{\text{attn}}) \odot \mathbf{Z}^p + (\alpha^n \mathbf{1}_{\text{attn}}) \odot \mathbf{Z}^n, \quad (6)$$

where $\alpha^p, \alpha^n \in \mathbb{R}^{(M+N) \times 1}$; $\mathbf{1}_{\text{attn}} \in \mathbb{R}^{1 \times d}$ is the all-ones vector; \odot denotes the Hadamard (element-wise) product; θ_3 is

the learned model parameters of ATTENTION; and each row of $\mathbf{Z} \in \mathbb{R}^{(M+N) \times d}$ indicates the embedding vector of each node in $\mathcal{U} \cup \mathcal{V}$.

Third, we turn to the optimization of model parameters $\{\theta_1, \theta_2, \theta_3\}$, which updates the embeddings \mathbf{Z} accordingly. In our study, we adopt the *BPR loss* [26], which has been widely used in recommender systems to comprehensively learn what users prefer from the historical user–item interactions. Nevertheless, simply applying the existing BPR loss to our setting does not precisely capture the relations of negatively connected neighbors; thus, we establish a *sign-aware* BPR loss, which is a new BPR-based loss that takes into account both positive and negative relations in the signed bipartite graph G^s , while accommodating the sign of edges in G^s as an indicator of what users like and dislike.

In the next section, we shall describe implementation details of the proposed SiReN method.

IV. PROPOSED SiReN METHOD

In this section, we elaborate on our SiReN method, designed for top- N recommendation. SiReN has the following three key components: 1) constructing a signed bipartite graph G^s for more precisely representing users' preferences, which is split into two graphs G^p and G^n with *positive* and *negative* edges each, 2) generating two embeddings \mathbf{Z}^p and \mathbf{Z}^n for the partitioned graphs with positive and negative edges via a GNN model and an MLP, respectively, and then using the attention model to learn the importance of \mathbf{Z}^p and \mathbf{Z}^n , and 3)

Algorithm 1 : SiReN

Input: G , w_o , $\Theta \triangleq \{\theta_1, \theta_2, \theta_3\}$, K (number of negative samples), λ_{reg} (regularization coefficient)

Output: \mathbf{Z}

- 1: **Initialization:** $\Theta \leftarrow$ random initialization
 - 2: /* Graph partitioning */
 - 3: Construction of G^s from G along with w_o
 - 4: Splitting G^s into G^p and G^n
 - 5: **while** not converged **do**
 - 6: Sample a batch \mathcal{D}_S from G^s with K negative samples
 - 7: **for** $\mathcal{D}'_S \subset \mathcal{D}_S$ **do**
 - 8: /* Generation of embeddings */
 - 9: $\mathbf{Z}^p \leftarrow \text{GNN}_{\theta_1}(G^p)$
 - 10: $\mathbf{Z}^n \leftarrow \text{MLP}_{\theta_2}(G^n)$
 - 11: $(\alpha^p, \alpha^n) \leftarrow \text{ATTENTION}_{\theta_3}(\mathbf{Z}^p, \mathbf{Z}^n)$
 - 12: $\mathbf{Z} \leftarrow (\alpha^p \mathbf{1}_{\text{attn}}) \odot \mathbf{Z}^p + (\alpha^n \mathbf{1}_{\text{attn}}) \odot \mathbf{Z}^n$
 - 13: /* Optimization */
 - 14: $\mathcal{L}_0 \leftarrow \text{sign-aware BPR loss}$
 - 15: $\mathcal{L} \leftarrow \mathcal{L}_0 + \lambda_{\text{reg}} \|\Theta\|^2$
 - 16: Update Θ by taking one step of gradient descent
 - 17: **end for**
 - 18: **end while**
 - 19: **return** \mathbf{Z}
-

establishing a sign-aware BPR loss function in the process of optimization. The overall procedure of the proposed SiReN method is summarized in Algorithm 1.

As one of main contributions to the design of our method, we start by constructing the signed bipartite graph G^s and then partitioning G^s into two edge-disjoint graphs G^p and G^n for exploiting the relation of positively and negatively connected neighbors.

In the following subsections, we explain how we discover embeddings of all nodes (i.e., users and items) and optimize our model via the sign-aware BPR loss during the training phase.

A. Network Architecture

In this subsection, we describe how to generate the embeddings of M users and N items in our SiReN method. As stated in Section III-B, SiReN basically contains three learning models, i.e., GNN_{θ_1} , MLP_{θ_2} , and $\text{ATTENTION}_{\theta_3}$. To generally indicate either users or items interchangeably, we denote a node in the graphs G^p and G^n , which can be in either \mathcal{U} or \mathcal{V} , by x .

First, we describe the GNN model, which is designed to be *model-agnostic*. To this end, we show a general form of the message passing mechanism [9], [10], [46] in which we iteratively update the representation of each node by aggregating representations of its neighbors using two functions, namely AGGREGATE_x^ℓ and UPDATE_x^ℓ , along with model parameters of GNN_{θ_1} in (3). Formally, at the ℓ -th layer of a GNN, AGGREGATE_x^ℓ aggregates (latent) feature information from the local neighborhood of node x in G^p at the $(\ell-1)$ -th GNN layer as follows:

$$\mathbf{m}_x^\ell \leftarrow \text{AGGREGATE}_x^\ell(\{\mathbf{h}_y^{\ell-1} | y \in \mathcal{N}_x \cup \{x\}\}), \quad (7)$$

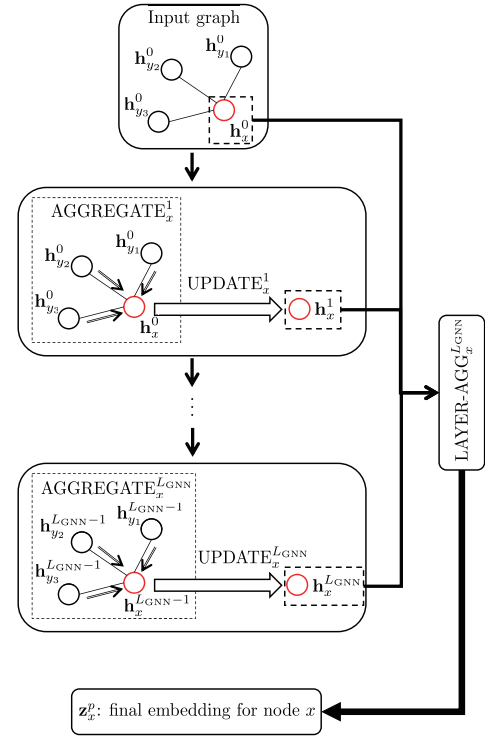


Fig. 3: The GNN architecture in our SiReN method, composed of three functions in (7)–(9).

where $\mathbf{h}_x^{\ell-1} \in \mathbb{R}^{1 \times d_{\text{GNN}}^{\ell-1}}$ denotes the $d_{\text{GNN}}^{\ell-1}$ -dimensional latent representation vector of node x at the $(\ell-1)$ -th GNN layer, \mathcal{N}_x is the set of neighbor nodes of x in G^p , and $\mathbf{m}_x^\ell \in \mathbb{R}^{1 \times d_{\text{GNN}}^\ell}$ is the aggregated information for node x at the ℓ -th GNN layer. Since x belongs to a node in either \mathcal{U} or \mathcal{V} , AGGREGATE_x^ℓ aggregates feature information of connected items if x is a user node, and vice versa. In the update step, we use UPDATE_x^ℓ to obtain the ℓ -th embedding vector \mathbf{h}_x^ℓ from the aggregated information \mathbf{m}_x^ℓ as follows:

$$\mathbf{h}_x^\ell \leftarrow \text{UPDATE}_x^\ell(x, \mathbf{m}_x^\ell). \quad (8)$$

We note that, for each node x , we randomly initialize the learnable 0-th embeddings (i.e., \mathbf{h}_x^0) due to the fact that we have no side information for users and items in our setting as in [18], [19]. Additionally, we present another function in our GNN model, namely $\text{LAYER-AGG}_x^{L_{\text{GNN}}}$, which performs *layer aggregation* similarly as in [47]. This operation is motivated by the argument that *oversmoothing* tends to occur in GNN-based recommender systems if the last GNN layer's embedding vectors are used as the final embedding \mathbf{Z}^p [48]. To alleviate the oversmoothing problem, we calculate the embedding vector $\mathbf{z}_x^p \in \mathbb{R}^{1 \times d}$ of node x via layer aggregation as follows:

$$\mathbf{z}_x^p \leftarrow \text{LAYER-AGG}_x^{L_{\text{GNN}}}(\{\mathbf{h}_x^\ell\}_{\ell=0}^{\ell=L_{\text{GNN}}}), \quad (9)$$

which results in the embeddings \mathbf{Z}^p for the graph G^p where L_{GNN} is the number of GNN layers. The GNN architecture of our SiReN method including the above three functions AGGREGATE_x^ℓ , UPDATE_x^ℓ , and $\text{LAYER-AGG}_x^{L_{\text{GNN}}}$ is illustrated in Fig. 3.

Remark 3. Now, let us state how the above three functions in (7)–(9) can be specified by several types of GNN-based recommender systems. As one state-of-the-art method, LR-GCCF [18] can be implemented by using

$$\text{AGGREGATE}_x^\ell = \sum_{y \in \mathcal{N}_x \cup \{x\}} \frac{1}{\sqrt{|\mathcal{N}_x| + 1} \sqrt{|\mathcal{N}_y| + 1}} \mathbf{h}_y^{\ell-1} \quad (10a)$$

$$\text{UPDATE}_x^\ell = \mathbf{m}_x^\ell \cdot W_{GNN}^\ell \quad (10b)$$

$$\text{LAYER-AGG}_x^{L_{GNN}} = \mathbf{h}_x^0 \parallel \mathbf{h}_x^1 \parallel \dots \parallel \mathbf{h}_x^{L_{GNN}}, \quad (10c)$$

where $W_{GNN}^\ell \in \mathbb{R}^{d_{GNN}^{\ell-1} \times d_{GNN}^\ell}$ is a learnable weight transformation matrix, \parallel is the concatenation operator, and L_{GNN} is the number of GNN layers. In addition, as another state-of-the-art method for recommendation, LightGCN [19] can be specified according to the following function setting:

$$\text{AGGREGATE}_x^\ell = \sum_{y \in \mathcal{N}_x} \frac{1}{\sqrt{|\mathcal{N}_x|} \sqrt{|\mathcal{N}_y|}} \mathbf{h}_y^{\ell-1} \quad (11a)$$

$$\text{UPDATE}_x^\ell = \mathbf{m}_x^\ell \quad (11b)$$

$$\text{LAYER-AGG}_x^{L_{GNN}} = \frac{1}{L_{GNN} + 1} \sum_{\ell=0}^{L_{GNN}} \mathbf{h}_x^\ell. \quad (11c)$$

Second, we pay our attention to the MLP architecture designed for the graph G^n having negative edges. We calculate the embeddings \mathbf{Z}^n using the MLP as follows:

$$\mathbf{Z}_\ell^n = \text{ReLU}(\mathbf{Z}_{\ell-1}^n W_{MLP}^\ell + \mathbf{1}_{MLP} \mathbf{b}_{MLP}^\ell) \quad (12a)$$

$$\mathbf{Z}^n = \mathbf{Z}_{L_{MLP}}^n, \quad (12b)$$

where $\ell = 1, 2, \dots, L_{MLP}$; L_{MLP} is the number of MLP layers; $\text{ReLU}(x) = \max(0, x)$; $W_{MLP}^\ell \in \mathbb{R}^{d_{MLP}^{\ell-1} \times d_{MLP}^\ell}$ is a learnable weight transformation matrix; $\mathbf{b}_{MLP}^\ell \in \mathbb{R}^{1 \times d_{MLP}^\ell}$ is a bias vector; d_{MLP}^ℓ is the dimension of the latent representation vector \mathbf{Z}_ℓ^n at the ℓ -th MLP layer; $\mathbf{1}_{MLP} \in \mathbb{R}^{(M+N) \times 1}$ is the all-ones vector; and $\mathbf{Z}_0^n \in \mathbb{R}^{(M+N) \times d_{MLP}^0}$ is the learnable 0-th layer's embedding matrix for all nodes in the set $\mathcal{U} \cup \mathcal{V}$, which is randomly initialized. That is, $\{W_{MLP}^\ell\}_{\ell=1}^{L_{MLP}}$, $\{\mathbf{b}_{MLP}^\ell\}_{\ell=1}^{L_{MLP}}$, and \mathbf{Z}_0^n correspond to the model parameters of MLP_{θ_2} in (4).

Third, we turn to describing the attention model. The importance (α^p, α^n) in (5) represents the attention values of two embeddings \mathbf{Z}^p and \mathbf{Z}^n for all nodes in $\mathcal{U} \cup \mathcal{V}$. Let us focus on node $x \in \mathcal{U} \cup \mathcal{V}$ whose embedding vectors calculated for the graphs G^p and G^n are given by $\mathbf{z}_x^p, \mathbf{z}_x^n \in \mathbb{R}^{1 \times d}$, respectively. Let w_x^p and w_x^n denote attention values of the two embeddings \mathbf{z}_x^p and \mathbf{z}_x^n , respectively, for node x . Then, our attention model learns a weight transformation matrix $W_{attn} \in \mathbb{R}^{d' \times d}$, an attention vector $\mathbf{q} \in \mathbb{R}^{d' \times 1}$, and a bias vector $\mathbf{b} \in \mathbb{R}^{d' \times 1}$ with a dimension d' , corresponding to the model parameters of $\text{ATTENTION}_{\theta_3}$ in (5), as follows:

$$w_x^p = \mathbf{q}^T \tanh(W_{attn} \mathbf{z}_x^p + \mathbf{b}) \quad (13a)$$

$$w_x^n = \mathbf{q}^T \tanh(W_{attn} \mathbf{z}_x^n + \mathbf{b}), \quad (13b)$$

where $\tanh(x) = \frac{\exp(x) - \exp(-x)}{\exp(x) + \exp(-x)}$ is the hyperbolic tangent activation function. By normalizing the attention values in (13a) and (13b) according to the softmax function, we have

$$\alpha_x^p = \frac{\exp(w_x^p)}{\exp(w_x^p) + \exp(w_x^n)} \quad (14a)$$

$$\alpha_x^n = \frac{\exp(w_x^n)}{\exp(w_x^p) + \exp(w_x^n)}, \quad (14b)$$

where α_x^p and α_x^n are the resulting importance of two embeddings \mathbf{z}_x^p and \mathbf{z}_x^n , respectively, which thus yields the final embedding $\mathbf{z}_x = \alpha_x^p \mathbf{z}_x^p + \alpha_x^n \mathbf{z}_x^n$ for each node x in (6).

B. Optimization

In this subsection, we explain the optimization of SiReN method in the training phase via our proposed loss function. We start by randomly initializing the learnable model parameters $\Theta = \{\theta_1, \theta_2, \theta_3\}$ in (3)–(5) (refer to line 1 in Algorithm 1). To train our learning models (i.e., the GNN, MLP, and attention models), we use a batch \mathcal{D}_S consisting of multiple samples of a triplet (u, i, j) , where $(u, i, w_{ui}^s) \in \mathcal{E}^s$ and $j \in \mathcal{V}$ is a negative sample (i.e., an unobserved item), which is not in the set of direct neighbors of user u in the signed bipartite graph G^s (refer to line 6).³ More specifically, we first acquire the set of edges, \mathcal{E}^s , in G^s and then sample K negative samples $\{j_n\}_{n=1}^K$ for each $(u, i, w_{ui}^s) \in \mathcal{E}^s$ in order to create new samples of a node triplet (u, i, j_n) for all $n \in \{1, \dots, K\}$, which yields the batch \mathcal{D}_S as follows:

$$\mathcal{D}_S = \{(u, i, j_n) \mid (u, i, w_{ui}^s) \in \mathcal{E}^s, j_n \notin \mathcal{N}_u, n \in \{1, \dots, K\}\}, \quad (15)$$

where \mathcal{N}_u is the set of neighbor nodes of user u in G^s . We further subsample mini-batches $\mathcal{D}'_S \subset \mathcal{D}_S$ to efficiently train our learning models (refer to line 7). The sampled triplets are fed into the loss function in the training loop along with the calculated embeddings \mathbf{Z} for all nodes in $\mathcal{U} \cup \mathcal{V}$ (refer to lines 9–12).

Now, we present our *sign-aware* BPR loss function, which is built upon the original BPR loss [26] widely used in recommender systems (see [14], [15], [17]–[19], [40], [42] and references therein). To this end, we define a user u 's *predicted preference* for an item i as the inner product of user and item final embeddings:

$$\hat{r}_{ui} \triangleq \mathbf{z}_u \mathbf{z}_i^T, \quad (16)$$

which is used for establishing our loss function.

However, simply employing the original BPR loss is not desirable in our setting since it is a pairwise loss based on the relative order between observed and unobserved items by basically assuming that high ratings are more reflective of a user's preferences with higher prediction values of \hat{r}_{ui} than the case of unobserved ones. On the other hand, our objective function should account for two types of observed items, which include both positive and negative relations between users and items, as well as unobserved ones. The proposed sign-aware BPR loss function is designed in such a way that

³For sampling $j \in \mathcal{V}$, we follow a negative sampling strategy using the degree-based unigram noise distribution [49], [50].

the predicted preference for an observed item (or its negative value when the observed item is negatively connected) is higher than its unobserved counterparts.

More formally, we define a ternary relation $>_u(i, j, w) \triangleq \{(i, j, w) | \hat{r}_{ui} > \hat{r}_{uj} \text{ if } w > 0 \text{ and } -\hat{r}_{ui} > \hat{r}_{uj} \text{ otherwise}\} \subset \mathcal{V} \times \mathcal{V} \times (\mathbb{R} \setminus \{0\})$. Based on the relation $>_u$, we aim at minimizing the following loss function \mathcal{L} for a given mini-batch \mathcal{D}'_S with the L_2 regularization:

$$\mathcal{L} = \mathcal{L}_0 + \lambda_{\text{reg}} \|\Theta\|^2, \quad (17)$$

where λ_{reg} is a hyperparameter that controls the L_2 regularization strength; Θ represents the model parameters; and \mathcal{L}_0 is the sign-aware BPR loss term realized by

$$\mathcal{L}_0 = - \sum_{(u, i, j) \in \mathcal{D}'_S} \log p(>_u(i, j, w_{ui}^s) | \Theta). \quad (18)$$

Here, to capture the above relation $>_u(i, j, w)$ for each $(u, i, j) \in \mathcal{D}'_S$, we model the likelihood in (18) as

$$p(>_u(i, j, w_{ui}^s) | \Theta) \triangleq \sigma(\text{sgn}(w_{ui}^s) \hat{r}_{ui} - \hat{r}_{uj}), \quad (19)$$

where $\text{sgn}(\cdot)$ is the sign function and $\sigma(x) = \frac{1}{1 + \exp(-x)}$ is the sigmoid function. By training our models through the loss in (17), it is possible to more elaborately learn representations of nodes depending on both positive and negative relations.

V. EXPERIMENTAL EVALUATION

In this section, we first describe real-world datasets used in the evaluation. We also present five competing methods including two baseline MF methods and three state-of-the-art GNN-based methods for comparison. After describing performance metrics and our experimental settings, we comprehensively evaluate the performance of our SiReN method and five benchmark methods. The source code for SiReN can be accessed via <https://github.com/woni-seo/SiReN-reco>.

A. Datasets

We conduct experiments on three real-world datasets, which are widely adopted for evaluating recommender systems. For all experiments, we use user–item interactions with ratings in each dataset as the input. The main statistics of each dataset, including the number of users, the number of items, the number of ratings, the density, and the rating scale, are summarized in Table II. In the following, we explain important characteristics of the datasets briefly.

MovieLens-1M (ML-1M)⁴. This is the most popular dataset in movie recommender systems, which consists of 5-star ratings (i.e., integer values from 1 to 5) of movies given by users [51].

Amazon-Book⁵. Among the Amazon-Review dataset containing product reviews and metadata, we select the Amazon-Book dataset, which consists of 5-star ratings [52]. We remove users/items that have less than 20 interactions similarly as in [53].

⁴<https://grouplens.org/datasets/movielens/1m/>.

⁵<https://jmcauley.ucsd.edu/data/amazon/index.html>.

Dataset	ML-1M	Amazon-Book	Yelp
# of users (M)	6,040	35,736	41,772
# of items (N)	3,952	38,121	30,037
# of ratings	1,000,209	1,960,674	2,116,215
Density (%)	4.19	0.14	0.16
Rating scale	1–5	1–5	1–5

TABLE II: Statistics of three real-world datasets.

Yelp⁶. This dataset is a local business review data consisting of 5-star ratings. As in the Amazon-Book dataset, we remove users/items that have less than 20 interactions.

B. Benchmark Methods

In this subsection, we present two baseline MF methods and three state-of-the-art GNN methods for comparison.

BPRMF [26]. This baseline method is a MF model optimized by the BPR loss, which assumes that each user prefers the items with which he/she has interacted to items with no interaction.

NeuMF [32]. As another popular baseline, NeuMF is a neural CF model, which generalizes standard MF and uses multiple hidden layers to generate user and item embeddings.

NGCF [15]. This state-of-the-art GNN-based approach follows basic operations inherited from the standard GCN [8] to explore the high-order connectivity information. More specifically, NGCF stacks embedding layers and concatenates embeddings obtained in all layers to constitute the final embeddings.

LR-GCCF [18]. LR-GCCF is a state-of-the-art GCN-based CF model. As two main characteristics, this model uses only linear transformation without nonlinear activation and concatenates all layers' embeddings to alleviate oversmoothing at deeper layers [48].

LightGCN [19]. LightGCN simplifies the design of GCN [8] to make the model more appropriate for recommendation by including only the most essential component such as neighborhood aggregation without nonlinear activation and weight transformation operations. Similarly as in LR-GCCF, this approach uses the weighted sum of embeddings learned at all layers as the final embedding.

C. Performance Metrics

To validate the performance of the proposed SiReN method and the five benchmark methods, we adopt three metrics, which are widely used to evaluate the accuracy of top- N recommendation. Let Te_u^+ and $R_u(N)$ denote the ground truth set (i.e., the set of items rated by user u in the test set) and the top- N recommendation list for user u , respectively. In the following, we describe each of metrics for recommendation accuracy.

The precision $P@N$ is defined as the ratio of relevant items to the set of recommended items and is expressed as

$$P@N = \frac{1}{M} \sum_{u \in \mathcal{U}} \frac{|Te_u^+ \cap R_u(N)|}{N}. \quad (20)$$

⁶<https://www.yelp.com/dataset>.

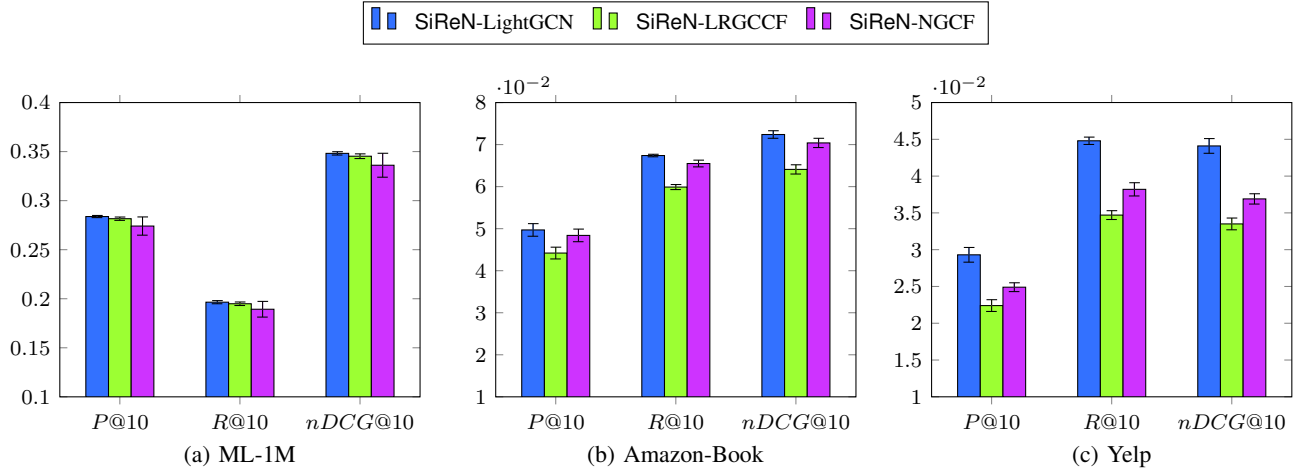


Fig. 4: Performance comparison according to different GNN models for each dataset in our SiReN method.

The recall $R@N$ is defined as the ratio of relevant items to the ground truth set and is expressed as

$$R@N = \frac{1}{M} \sum_{u \in \mathcal{U}} \frac{|Te_u^+ \cap R_u(N)|}{|Te_u^+|}. \quad (21)$$

The normalized discounted cumulative gain $nDCG@N$ [54] measures a ranking quality of the recommendation list by assigning higher scores to relevant items at top- N ranking positions in the list:

$$nDCG@N = \frac{1}{M} \sum_{u \in \mathcal{U}} nDCG_u@N. \quad (22)$$

Let y_k be the binary relevance of the k -th item i_k in $R_u(N)$ for each user u : $y_k = 1$ if $i_k \in Te_u^+$ and 0 otherwise. Then, $nDCG_u@N$ can be computed as

$$nDCG_u@N = \frac{DCG_u@N}{IDCG_u@N}, \quad (23)$$

where $DCG_u@N$ is

$$DCG_u@N = \sum_{i=1}^N \frac{2^{y_i} - 1}{\log_2(i+1)} \quad (24)$$

and $IDCG_u@N$ indicates the ideal case of $DCG_u@N$ (i.e., all relevant items are at the top rank in $R_u(N)$). Note that all metrics are in a range of $[0, 1]$, and higher values represent better performance.

D. Experimental Setup

In this subsection, we describe the experimental settings of neural networks in our SiReN method. We implement SiReN via PyTorch Geometric [55], which is a geometric deep learning extension library in PyTorch. In our experiments, we adopt GNN models for the graph G^p with positive edges and the 2-layer MLP architecture for the graph G^n with negative edges. We use the Xavier initializer [56] to initialize the model parameters $\Theta = \{\theta_1, \theta_2, \theta_3\}$. We use dropout regularization [57] with the probability of 0.5 for the MLP and attention models in (4) and (5). We set the dimension of

the embedding space and all hidden latent spaces to 64; the number of negative samples, K , to 40; and the strength of L_2 regularization, λ_{reg} , to 0.1 for the ML-1M dataset and 0.05 for the Amazon-Book and Yelp datasets. We train our model using the Adam optimizer [58] with a learning rate of 0.005.

For each dataset, we conduct 5-fold cross-validation by splitting it into two subsets: 80% of the ratings (i.e., user-item interactions) as the training set and 20% of the ratings as the test set. In the training set, when we implement five benchmark methods, we regard only the items with the rating scores of 4 and 5 as observed interactions by removing the ratings whose scores are lower than 4 as in [7], [40], [42]; however, when we implement our SiReN method, we utilize all user-item interactions including low ratings in the training set while the parameter w_o , indicating the design criterion for signed bipartite graph construction, is set to 3.5.⁷ It is worthwhile to note that, for fair comparison, the test set consists of only the ratings of 4 and 5 as the *ground truth* set for all the methods including SiReN.

E. Experimental Results

In this subsection, our empirical study is designed to answer the following four key research questions.

- RQ1.** How do underlying GNN models affect the performance of the SiReN method?
- RQ2.** Which model architecture is appropriate to the graph G^n with negative edges?
- RQ3.** How much does the SiReN method improve the top- N recommendation over baseline and state-of-the-art methods?
- RQ4.** How robust is our SiReN method with respect to interaction sparsity levels?

To answer these research questions, we comprehensively carry out experiments in the following.

⁷Our empirical findings reveal that such a setting in SiReN consistently leads to superior performance to that of other values of w_o for all datasets having the 1-5 rating scale.

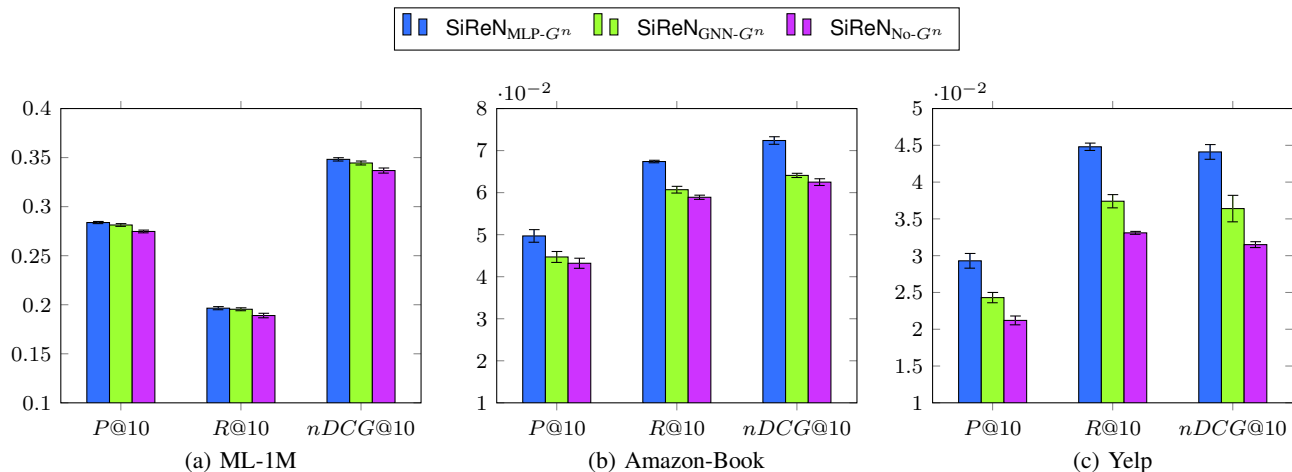


Fig. 5: Performance comparison according to several model architectures used for the graph G^n for each dataset in our SiReN method.

a) Comparative Study Among GNN Models Used for G^p (RQ1): In Fig. 4, for all datasets, we evaluate the accuracy of top- N recommendation in terms of $P@N$, $R@N$, and $nDCG@N$ when N is set to 10 while using various GNN models used for the graph G^p in our SiReN method. Since our method is GNN-model-agnostic, any existing GNN models can be adopted; however, in our experiments, we adopt three state-of-the-art GNN models that exhibit superior performance in recommender systems from the literature, namely NGCF [15] (SiReN-NGCF), LR-GCCF [18] (SiReN-LRGCCF), and LightGCN [19] (SiReN-LightGCN). From Fig. 4, we observe that SiReN-LightGCN consistently outperforms other models for all performance metrics. As discussed in [19], this is because nonlinear activation and weight transformation operations in GNNs rather tend to degrade the recommendation accuracy; LightGCN thus attempted to simplify the design of GCN by removing such operations. It turns out that such a gain achieved by LightGCN is also possible in our SiReN model that contains three learning models including the GNN, MLP, and attention models.

From these findings, we use SiReN-LightGCN in our subsequent experiments unless otherwise stated.

b) Comparative Study Among Model Architectures Used for G^n (RQ2): We perform another comparative study among model architectures used for the graph G^n with negative edges. We adopted the MLP for G^n since negative edges in G^n can undermine the assortativity and thus message passing to such dissimilar nodes would not be feasible. In this experiment, we empirically validate this claim by taking into account two other design scenarios. We evaluate the accuracy of top- N recommendation when N is set to 10 for all datasets. First, we recall the original SiReN method employing MLP for G^n , dubbed SiReN_{MLP-Gⁿ}.

Second, instead of employing MLP, we introduce SiReN_{GNN-Gⁿ} that uses an additional GNN model for the graph G^n to calculate the embedding vectors \mathbf{Z}^n :

$$\mathbf{Z}^n = \text{GNN}_{\theta'_1}(G^n), \quad (25)$$

where θ'_1 is the learned model parameters of GNN for the graph G^n . In this experiment, we adopt LightGCN [19] among GNN models.

Third, as an ablation study, we introduce SiReN_{No-Gⁿ} that does not calculate the embedding vectors \mathbf{Z}^n . In other words, we only use the embedding vectors \mathbf{Z}^p in (3) as the final embeddings \mathbf{Z} in (6) (i.e., $\mathbf{Z} = \mathbf{Z}^p$). Note that SiReN_{No-Gⁿ} is identical to the model architecture of LightGCN [19], which generates embedding vectors by aggregating only the information of positively connected neighbors. However, unlike LightGCN, SiReN_{No-Gⁿ} utilizes the sign-aware BPR loss in (17)–(19) as our objective function in the process of optimization.

From Fig. 5, our findings are as follows:

- SiReN_{MLP-Gⁿ} is always superior to SiReN_{GNN-Gⁿ} regardless of performance metrics, which indeed validates our claim addressed in Remark 1.
- SiReN_{No-Gⁿ} is even inferior to SiReN_{GNN-Gⁿ}. This implies that, although the model in SiReN_{No-Gⁿ} is trained via our sign-aware BPR loss, both positive and negative relations in the signed bipartite graph G^s are not precisely captured during training unless an appropriate model architecture is designed for the graph G^n .

From these findings, we use SiReN_{MLP-Gⁿ} in our subsequent experiments unless otherwise stated.

c) Comparison With Benchmark Methods (RQ3): The performance comparison between our SiReN method and three state-of-the-art GNN methods, including NGCF [15], LR-GCCF [18], and LightGCN [19], as well as two baseline MF methods, including BPRMF [26] and NeuMF [32], for top- N recommendation is comprehensively presented in Table III with respect to three performance metrics using three real-world datasets, where $N \in \{10, 15, 20\}$. We note that the hyperparameters in all the aforementioned benchmark methods are tuned differently according to each dataset so as to provide the best performance. In Table III, the value with an underline indicates the best performer for each case. We would like to make the following insightful observations:

Dataset	Method	$N = 10$			$N = 15$			$N = 20$		
		$P@N$	$R@N$	$nDCG@N$	$P@N$	$R@N$	$nDCG@N$	$P@N$	$R@N$	$nDCG@N$
ML-1M	BPRMF	0.1999±0.0044	0.1227±0.0019	0.2363±0.0063	0.1772±0.0033	0.1608±0.0016	0.2314±0.0053	0.1615±0.0027	0.1930±0.0021	0.2321±0.0050
	NeuMF	0.2397±0.0030	0.1599±0.0011	0.2847±0.0035	0.2138±0.0027	0.2098±0.0023	0.2827±0.0032	0.1956±0.0025	0.2513±0.0028	0.2861±0.0032
	NGCF	0.2477±0.0023	0.1748±0.0025	0.3031±0.0033	0.2174±0.0022	0.2229±0.0027	0.2985±0.0029	0.1960±0.0020	0.2627±0.0026	0.3002±0.0030
	LR-GCCF	0.2539±0.0027	0.1802±0.0031	0.3117±0.0039	0.2220±0.0025	0.2292±0.0046	0.3066±0.0042	0.1998±0.0024	0.2687±0.0046	0.3079±0.0045
	LightGCN	0.2679±0.0013	0.1909±0.0016	0.3297±0.0018	0.2349±0.0016	0.2432±0.0029	0.3249±0.0022	0.2109±0.0013	0.2837±0.0025	0.3258±0.0021
	SiReN	<u>0.2838±0.0011</u>	<u>0.1965±0.0016</u>	<u>0.3482±0.0017</u>	<u>0.2480±0.0008</u>	<u>0.2489±0.0013</u>	<u>0.3415±0.0015</u>	<u>0.2228±0.0009</u>	<u>0.2909±0.0016</u>	<u>0.3419±0.0017</u>
Amazon-Book	BPRMF	0.0263±0.0033	0.0365±0.0057	0.0371±0.0053	0.0243±0.0029	0.0500±0.0074	0.0419±0.0058	0.0228±0.0027	0.0621±0.0090	0.0461±0.0064
	NeuMF	0.0339±0.0018	0.0452±0.0010	0.0483±0.0018	0.0303±0.0014	0.0597±0.0012	0.0530±0.0017	0.0277±0.0012	0.0722±0.0012	0.0573±0.0017
	NGCF	0.0391±0.0014	0.0532±0.0008	0.0562±0.0010	0.0403±0.0127	0.0706±0.0007	0.0618±0.0009	0.0321±0.0009	0.0858±0.0007	0.0671±0.0008
	LR-GCCF	0.0399±0.0014	0.0544±0.0005	0.0574±0.0009	0.0357±0.0013	0.0721±0.0004	0.0631±0.0008	0.0327±0.0012	0.0874±0.0004	0.0684±0.0009
	LightGCN	0.0443±0.0013	0.0595±0.0008	0.0638±0.0007	0.0393±0.0011	0.0781±0.0008	0.0698±0.0007	0.0358±0.0010	0.0942±0.0009	0.0753±0.0006
	SiReN	<u>0.0497±0.0015</u>	<u>0.0674±0.0003</u>	<u>0.0724±0.0009</u>	<u>0.0438±0.0015</u>	<u>0.0878±0.0003</u>	<u>0.0788±0.0001</u>	<u>0.0397±0.0013</u>	<u>0.1049±0.0005</u>	<u>0.0846±0.0012</u>
Yelp	BPRMF	0.0116±0.0014	0.0180±0.0020	0.0165±0.0017	0.0111±0.0013	0.0257±0.0026	0.0194±0.0021	0.0107±0.0013	0.0329±0.0033	0.0221±0.0024
	NeuMF	0.0174±0.0009	0.0262±0.0017	0.0254±0.0015	0.0159±0.0007	0.0358±0.0019	0.0288±0.0016	0.0149±0.0006	0.0445±0.0023	0.0319±0.0017
	NGCF	0.0243±0.0009	0.0383±0.0010	0.0368±0.0010	0.0219±0.0007	0.0515±0.0008	0.0413±0.0009	0.0202±0.0007	0.0632±0.0009	0.0455±0.0009
	LR-GCCF	0.0258±0.0010	0.0405±0.0009	0.0392±0.0011	0.0232±0.0008	0.0543±0.0010	0.0439±0.0012	0.0214±0.0007	0.0665±0.0012	0.0481±0.0013
	LightGCN	0.0281±0.0009	0.0435±0.0007	0.0427±0.0008	0.0251±0.0008	0.0582±0.0010	0.0476±0.0008	0.0231±0.0007	0.0711±0.0011	0.0521±0.0009
	SiReN	<u>0.0293±0.0010</u>	<u>0.0448±0.0005</u>	<u>0.0441±0.0010</u>	<u>0.0262±0.0009</u>	<u>0.0600±0.0006</u>	<u>0.0492±0.0010</u>	<u>0.0241±0.0008</u>	<u>0.0731±0.0005</u>	<u>0.0537±0.0010</u>

TABLE III: Performance comparison among SiReN and five benchmark methods in terms of three performance metrics (average \pm standard deviation) when $N \in \{10, 15, 20\}$. Here, the best method for each case is highlighted using underlines.

Group	Method	$N = 10$			$N = 15$			$N = 20$		
		$P@N$	$R@N$	$nDCG@N$	$P@N$	$R@N$	$nDCG@N$	$P@N$	$R@N$	$nDCG@N$
[0, 20) (405.4)	BPRMF	0.0485±0.0056	0.1348±0.0200	0.1046±0.0148	0.0433±0.0031	0.1810±0.0145	0.1223±0.0128	0.0384±0.0017	0.2121±0.0133	0.1333±0.0123
	NeuMF	0.0675±0.0050	0.1873±0.0182	0.1449±0.0147	0.0576±0.0036	0.2397±0.0204	0.1653±0.0149	0.0505±0.0023	0.2808±0.0159	0.1794±0.0135
	NGCF	0.0760±0.0040	0.2141±0.0126	0.1679±0.0129	0.0638±0.0015	0.2660±0.0100	0.1884±0.0101	0.0553±0.0014	0.3074±0.0102	0.2028±0.0095
	LR-GCCF	0.0776±0.0037	0.2148±0.0145	0.1736±0.0162	0.0643±0.0025	0.2670±0.0139	0.1938±0.0147	0.0555±0.0023	0.3070±0.0175	0.2077±0.0161
	LightGCN	0.0832±0.0029	0.2326±0.0116	0.1847±0.0108	0.0690±0.0028	0.2878±0.0146	0.2063±0.0108	0.0592±0.0011	0.3272±0.0130	0.2202±0.0102
	SiReN	<u>0.0826±0.0041</u>	<u>0.2289±0.0120</u>	<u>0.1836±0.0114</u>	<u>0.0679±0.0023</u>	<u>0.2810±0.0120</u>	<u>0.2040±0.0108</u>	<u>0.0580±0.0025</u>	<u>0.3211±0.0176</u>	<u>0.2178±0.0126</u>
[20, 50) (1773)	BPRMF	0.0731±0.0018	0.1358±0.0026	0.1194±0.0041	0.0635±0.0013	0.1773±0.0046	0.1364±0.0037	0.0571±0.0011	0.2121±0.0036	0.1502±0.0034
	NeuMF	0.1010±0.0020	0.1916±0.0052	0.1679±0.0038	0.0877±0.0014	0.2485±0.0061	0.1913±0.0041	0.0784±0.0009	0.2944±0.0064	0.2096±0.0045
	NGCF	0.1149±0.0021	0.2198±0.0073	0.1961±0.0060	0.0959±0.0015	0.2727±0.0086	0.2177±0.0061	0.0843±0.0005	0.3175±0.0051	0.2356±0.0047
	LR-GCCF	0.1193±0.0026	0.2298±0.0050	0.2062±0.0048	0.0993±0.0022	0.2844±0.0077	0.2284±0.0055	0.0866±0.0021	0.3276±0.0076	0.2458±0.0058
	LightGCN	0.1262±0.0020	0.2424±0.0044	0.2194±0.0037	0.1055±0.0015	0.3013±0.0055	0.2434±0.0036	0.0914±0.0013	0.3455±0.0062	0.2611±0.0039
	SiReN	<u>0.1285±0.0013</u>	<u>0.2438±0.0035</u>	<u>0.2238±0.0031</u>	<u>0.1068±0.0013</u>	<u>0.3006±0.0042</u>	<u>0.2470±0.0035</u>	<u>0.0925±0.0010</u>	<u>0.3453±0.0041</u>	<u>0.2650±0.0035</u>
[50, ∞) (3861.6)	BPRMF	0.2722±0.0068	0.1156±0.0035	0.3021±0.0083	0.2418±0.0052	0.1514±0.0037	0.2852±0.0071	0.2208±0.0044	0.1825±0.0043	0.2789±0.0067
	NeuMF	0.3194±0.0055	0.1430±0.0033	0.3514±0.0066	0.2862±0.0043	0.1893±0.0037	0.3355±0.0059	0.2629±0.0038	0.2290±0.0041	0.3312±0.0056
	NGCF	0.3247±0.0040	0.1505±0.0031	0.3649±0.0052	0.2875±0.0039	0.1962±0.0037	0.3459±0.0052	0.2604±0.0032	0.2335±0.0034	0.3390±0.0047
	LR-GCCF	0.3321±0.0033	0.1544±0.0030	0.3730±0.0046	0.2930±0.0031	0.2006±0.0032	0.3531±0.0043	0.2652±0.0028	0.2383±0.0033	0.3459±0.0043
	LightGCN	0.3502±0.0026	0.1635±0.0029	0.3898±0.0109	0.3098±0.0024	0.2125±0.0034	0.3736±0.0043	0.2798±0.0020	0.2516±0.0035	0.3656±0.0042
	SiReN	<u>0.3738±0.0014</u>	<u>0.1720±0.0025</u>	<u>0.4208±0.0025</u>	<u>0.3296±0.0014</u>	<u>0.2224±0.0024</u>	<u>0.3978±0.0028</u>	<u>0.2979±0.0015</u>	<u>0.2634±0.0029</u>	<u>0.3890±0.0031</u>

TABLE IV: Performance comparison among SiReN and five benchmark methods in terms of three performance metrics (average \pm standard deviation) for the ML-1M dataset according to three different user groups. For each user group, the number in the parentheses indicates the average number of users in the belonging group. Here, the best method for each case is highlighted using underlines.

- Our SiReN method consistently outperforms five benchmark methods for all datasets regardless of the performance metrics and the values of N . The superiority of our method comes from the fact that we are capable of more precisely representing users' preferences without any information loss. This implies that low ratings are indeed informative as long as the low rating information is well exploited through judicious model design and optimization.
- The second best performer is LightGCN for all the cases. The performance gap between our SiReN method (X) and the second best performer (Y) is the largest when the Amazon-Book dataset is used; the maximum improvement rates of 12.19%, 13.28%, and 13.48% are achieved in terms of $P@10$, $R@10$, and $nDCG@10$, respectively, where the improvement rate (%) is given by $\frac{X-Y}{Y} \times 100$. We recall that the Amazon-Book dataset has the lowest density (i.e., the highest sparsity) out of three datasets (refer to Table II). Thus, from the above empirical finding, it is seen that exploiting negative user-item interactions in sparser datasets would be more beneficial and effective in improving the recommendation accuracy.
- Two baseline MF methods reveal worse performance than that of three state-of-the-art GNN methods. This indicates that exploring the high-order connectivity information via GNNs indeed significantly improves the recommendation

Group	Method	N = 10			N = 15			N = 20		
		P@N	R@N	nDCG@N	P@N	R@N	nDCG@N	P@N	R@N	nDCG@N
[0, 20] (8651.8)	BPRMF	0.0157±0.0021	0.0455±0.0080	0.0330±0.0054	0.0142±0.0019	0.0619±0.0103	0.0393±0.0062	0.0132±0.0017	0.0760±0.0123	0.0442±0.0069
	NeuMF	0.0199±0.0016	0.0542±0.0013	0.0420±0.0020	0.0171±0.0012	0.0699±0.0017	0.0482±0.0021	0.0154±0.0001	0.0839±0.0020	0.0532±0.0021
	NGCF	0.0235±0.0012	0.0649±0.0019	0.0497±0.0014	0.0204±0.0011	0.0848±0.0015	0.0576±0.0013	0.0183±0.0010	0.1019±0.0008	0.0636±0.0012
	LR-GCCF	0.0241±0.0013	0.0665±0.0013	0.0508±0.0009	0.0208±0.0012	0.0863±0.0010	0.0586±0.0009	0.0188±0.0011	0.1042±0.0012	0.0649±0.0011
	LightGCN	0.0258±0.0011	0.0712±0.0021	0.0551±0.0008	0.0224±0.0011	0.0923±0.0022	0.0635±0.0009	0.0200±0.0010	0.1102±0.0023	0.0697±0.0010
	SiReN	<u>0.0304±0.0021</u>	<u>0.0824±0.0010</u>	<u>0.0652±0.0015</u>	<u>0.0258±0.0018</u>	<u>0.1053±0.0013</u>	<u>0.0743±0.0018</u>	<u>0.0228±0.0015</u>	<u>0.1244±0.0013</u>	<u>0.0811±0.0018</u>
[20, 50] (19006.2)	BPRMF	0.0211±0.0026	0.0371±0.0058	0.0320±0.0046	0.0194±0.0023	0.0508±0.0077	0.0383±0.0055	0.0181±0.0021	0.0633±0.0092	0.0435±0.0060
	NeuMF	0.0281±0.0019	0.0468±0.0008	0.0426±0.0015	0.0249±0.0016	0.0622±0.0010	0.0497±0.0015	0.0225±0.0013	0.0749±0.0011	0.0551±0.0016
	NGCF	0.0322±0.0016	0.0547±0.0007	0.0494±0.0008	0.0286±0.0014	0.0727±0.0009	0.0576±0.0009	0.0261±0.0012	0.0885±0.0012	0.0642±0.0009
	LR-GCCF	0.0330±0.0016	0.0560±0.0007	0.0507±0.0007	0.0292±0.0014	0.0744±0.0006	0.0591±0.0007	0.0265±0.0013	0.0900±0.0006	0.0656±0.0008
	LightGCN	0.0364±0.0016	0.0615±0.0009	0.0562±0.0005	0.0319±0.0014	0.0807±0.0009	0.0650±0.0005	0.0288±0.0013	0.0971±0.0012	0.0719±0.0006
	SiReN	<u>0.0414±0.0018</u>	<u>0.0696±0.0008</u>	<u>0.0643±0.0007</u>	<u>0.0361±0.0018</u>	<u>0.0906±0.0003</u>	<u>0.0740±0.0010</u>	<u>0.0323±0.0016</u>	<u>0.1082±0.0003</u>	<u>0.0814±0.0011</u>
[50, ∞) (8078)	BPRMF	0.0497±0.0058	0.0255±0.0034	0.0533±0.0063	0.0466±0.0052	0.0357±0.0046	0.0527±0.0062	0.0439±0.0049	0.0449±0.0057	0.0543±0.0065
	NeuMF	0.0625±0.0026	0.0318±0.0007	0.0683±0.0030	0.0570±0.0023	0.0433±0.0008	0.0658±0.0025	0.0530±0.0017	0.0536±0.0006	0.0669±0.0020
	NGCF	0.0718±0.0020	0.0371±0.0003	0.0789±0.0019	0.0652±0.0014	0.0505±0.0004	0.0761±0.0012	0.0609±0.0013	0.0626±0.0007	0.0777±0.0009
	LR-GCCF	0.0729±0.0022	0.0378±0.0002	0.0799±0.0026	0.0665±0.0019	0.0515±0.0004	0.0774±0.0020	0.0618±0.0018	0.0636±0.0006	0.0787±0.0018
	LightGCN	0.0823±0.0021	0.0423±0.0003	0.0911±0.0025	0.0747±0.0018	0.0574±0.0004	0.0877±0.0018	0.0692±0.0016	0.0707±0.0007	0.0889±0.0015
	SiReN	<u>0.0896±0.0017</u>	<u>0.0463±0.0005</u>	<u>0.0988±0.0018</u>	<u>0.0808±0.0018</u>	<u>0.0623±0.0006</u>	<u>0.0947±0.0016</u>	<u>0.0747±0.0018</u>	<u>0.0764±0.0006</u>	<u>0.0960±0.0015</u>

TABLE V: Performance comparison among SiReN and five benchmark methods in terms of three performance metrics (average \pm standard deviation) for the Amazon-Book dataset according to three different user groups. For each user group, the number in the parentheses indicates the average number of users in the belonging group. Here, the best method for each case is highlighted using underlines.

Group	Method	N = 10			N = 15			N = 20		
		P@N	R@N	nDCG@N	P@N	R@N	nDCG@N	P@N	R@N	nDCG@N
[0, 20] (10469.8)	BPRMF	0.0061±0.0009	0.0197±0.0024	0.0132±0.0018	0.0057±0.0008	0.0276±0.0031	0.0161±0.0022	0.0055±0.0008	0.0352±0.0036	0.0187±0.0024
	NeuMF	0.0083±0.0009	0.0268±0.0024	0.0189±0.0020	0.0075±0.0007	0.0364±0.0026	0.0224±0.0021	0.0069±0.0006	0.0453±0.0031	0.0254±0.0022
	NGCF	0.0128±0.0010	0.0413±0.0017	0.0295±0.0016	0.0114±0.0009	0.0552±0.0014	0.0347±0.0016	0.0104±0.0008	0.0679±0.0016	0.0388±0.0017
	LR-GCCF	0.0134±0.0013	0.0434±0.0023	0.0310±0.0022	0.0120±0.0001	0.0584±0.0022	0.0366±0.0021	0.0109±0.0008	0.0710±0.0025	0.0408±0.0023
	LightGCN	0.0144±0.0010	0.0462±0.0012	0.0332±0.0015	0.0127±0.0009	0.0615±0.0014	0.0389±0.0016	0.0116±0.0008	0.0749±0.0015	0.0434±0.0016
	SiReN	<u>0.0145±0.0011</u>	<u>0.0468±0.0012</u>	<u>0.0333±0.0012</u>	<u>0.0129±0.0010</u>	<u>0.0629±0.0016</u>	<u>0.0393±0.0014</u>	<u>0.0117±0.0008</u>	<u>0.0759±0.0017</u>	<u>0.0436±0.0015</u>
[20, 50] (22866.2)	BPRMF	0.0094±0.0014	0.0183±0.0019	0.0146±0.0016	0.0090±0.0012	0.0263±0.0025	0.0181±0.0019	0.0086±0.0012	0.0335±0.0034	0.0210±0.0024
	NeuMF	0.0137±0.0008	0.0267±0.0017	0.0222±0.0013	0.0124±0.0008	0.0365±0.0020	0.0265±0.0015	0.0116±0.0007	0.0451±0.0023	0.0300±0.0015
	NGCF	0.0198±0.0010	0.0392±0.0011	0.0329±0.0009	0.0177±0.0009	0.0526±0.0010	0.0388±0.0009	0.0163±0.0008	0.0645±0.0013	0.0435±0.0010
	LR-GCCF	0.0208±0.0011	0.0413±0.0007	0.0348±0.0008	0.0186±0.0009	0.0552±0.0010	0.0409±0.0009	0.0171±0.0009	0.0677±0.0011	0.0458±0.0010
	LightGCN	0.0224±0.0012	0.0443±0.0008	0.0377±0.0009	0.0200±0.0010	0.0592±0.0013	0.0442±0.0009	0.0183±0.0009	0.0724±0.0015	0.0494±0.0010
	SiReN	<u>0.0231±0.0013</u>	<u>0.0455±0.0007</u>	<u>0.0387±0.0012</u>	<u>0.0206±0.0011</u>	<u>0.0607±0.0006</u>	<u>0.0454±0.0013</u>	<u>0.0189±0.0009</u>	<u>0.0741±0.0005</u>	<u>0.0507±0.0013</u>
[50, ∞) (8436)	BPRMF	0.0241±0.0024	0.0150±0.0015	0.0256±0.0020	0.0236±0.0025	0.0221±0.0024	0.0269±0.0024	0.0229±0.0022	0.0286±0.0028	0.0292±0.0025
	NeuMF	0.0384±0.0018	0.0240±0.0014	0.0420±0.0023	0.0352±0.0013	0.0331±0.0014	0.0423±0.0020	0.0331±0.0010	0.0416±0.0018	0.0447±0.0021
	NGCF	0.0506±0.0016	0.0323±0.0004	0.0562±0.0017	0.0458±0.0012	0.0439±0.0003	0.0562±0.0012	0.0425±0.0010	0.0542±0.0004	0.0588±0.0011
	LR-GCCF	0.0542±0.0012	0.0346±0.0003	0.0608±0.0014	0.0492±0.0013	0.0470±0.0006	0.0606±0.0013	0.0455±0.0010	0.0579±0.0005	0.0633±0.0011
	LightGCN	0.0599±0.0013	0.0380±0.0004	0.0675±0.0012	0.0540±0.0013	0.0514±0.0004	0.0670±0.0008	0.0497±0.0011	0.0631±0.0003	0.0696±0.0006
	SiReN	<u>0.0639±0.0016</u>	<u>0.0406±0.0006</u>	<u>0.0718±0.0018</u>	<u>0.0574±0.0012</u>	<u>0.0547±0.0005</u>	<u>0.0713±0.0013</u>	<u>0.0529±0.0014</u>	<u>0.0670±0.0008</u>	<u>0.0740±0.0014</u>

TABLE VI: Performance comparison among SiReN and five benchmark methods in terms of three performance metrics (average \pm standard deviation) for the Yelp dataset according to three different user groups. For each user group, the number in the parentheses indicates the average number of users in the belonging group. Here, the best method for each case is highlighted using underlines.

accuracy.

- The gain of LightGCN over LR-GCCF and NGCF is consistently observed. We note that, in contrast to LR-GCCF and NGCF, LightGCN aggregates the information of neighbors without both nonlinear activation and weight transformation operations. Our experimental results coincide with the argument in [19] that a simple aggregator of the information of neighbors using a weighted sum is the most effective as long as GNN-based recommender systems are associated.

d) Robustness to Interaction Sparsity Levels (RQ4):

Needless to say, the sparsity issue is one of crucial challenges on designing recommender systems since few user-item interactions are insufficient to generate high-quality embeddings [15], [35]. In this experiment, we demonstrate that making use of low rating scores for better representing users' preferences enables us to alleviate this sparsity issue. To this end, we partition the set of users in the test set into three groups according to the number of interactions in the training set as in [15], [35]. More precisely, for each dataset, we split the users into three groups, each of which is composed of

the users whose number of interactions in the training set ranges between $[0, 20)$, $[20, 50)$, and $[50, \infty)$, respectively. In Tables IV–VI, we comprehensively carry out the performance comparison between our SiReN method and five benchmark methods with respect to three performance metrics of top- N recommendation using the ML-1M, Amazon-Book, and Yelp datasets, respectively, where experimental results are shown according to three interaction sparsity levels for each dataset. Our findings can be summarized as follows:

- Our SiReN method almost consistently outperforms benchmark methods except for only one case of user groups in the ML-1M dataset. This comes from the fact that the ML-1M dataset is relatively less sparse; thus, in this case, exploiting the set of negative interactions in designing GNN-based recommender systems may not be often useful in improving the recommendation accuracy.
- The performance gap between our SiReN method and the second best performer is the largest for the user group having $[0, 20)$ interactions in the Amazon-Book dataset (refer to Table V); the maximum improvement rates of 17.83%, 15.73%, and 18.33% are achieved in terms of $P@10$, $R@10$, and $nDCG@10$, respectively. As stated above, the performance improvement of SiReN over competing methods is significant when sparse datasets are used.
- As the number of interactions per user increases, the performance is likely to be enhanced for all the methods regardless of types of datasets. It is obvious that more user–item interactions yield higher recommendation accuracy.

VI. CONCLUDING REMARKS

In this paper, we explored a fundamentally important problem of how to take advantage of both high and low rating scores in developing GNN-based recommender systems. To tackle this challenge, we introduced a novel method, termed SiReN, that is designed based on sign-aware learning and optimization models along with a GNN architecture. Specifically, we presented an approach to 1) constructing a signed bipartite graph G^s to distinguish users’ positive and negative feedback and then partitioning G^s into two edge-disjoint graphs G^p and G^n with positive and negative edges each, respectively, 2) generating two embeddings for G^p and G^n via a GNN model and an MLP, respectively, and then using an attention model to discover the final embeddings, and 3) training our learning models by establishing a sign-aware BPR loss function that captures each relation of positively and negatively connected neighbors. Using three real-world datasets, we demonstrated that our SiReN method remarkably outperforms three state-of-the-art GNN methods as well as two baseline MF methods while showing gains over the second best performer (i.e., LightGCN) by up to 13.48% in terms of the recommendation accuracy. We also demonstrated that our proposed method is robust to more challenging situations according to interaction sparsity levels by investigating that the performance improvement of SiReN over state-of-the-art methods is significant when sparse datasets are used. Additionally, we empirically

showed the effectiveness of MLP used for the graph G^n with negative edges.

Potential avenues of future research include the design of a more sophisticated GNN model that fits well into G^n in signed bipartite graphs. Here, the challenges lie in developing a new information aggregation and propagation mechanism.

ACKNOWLEDGMENT

This research was supported by the National Research Foundation of Korea (NRF) grant funded by the Korea government (MSIT) (No. 2021R1A2C3004345), by the Institute of Information & Communications Technology Planning & Evaluation (IITP) grant funded by the Korea Government (MSIT) (No. 2020-0-01441, Artificial Intelligence Convergence Research Center (Chungnam National University)), and by the Yonsei University, Republic of Korea Research Fund of 2021 (2021-22-0083). The authors would like to thank Dr. Hajoon Ko from Harvard University for his helpful comments.

REFERENCES

- [1] C.-K. Hsieh, L. Yang, Y. Cui, T.-Y. Lin, S. Belongie, and D. Estrin, “Collaborative metric learning,” in *Proc. 26th Int. Conf. World Wide Web (WWW’17)*, Perth, Aust., Apr. 2017, pp. 193–201.
- [2] T. Ebesu, B. Shen, and Y. Fang, “Collaborative memory network for recommendation systems,” in *Proc. 41st Int. ACM SIGIR Conf. Res. Develop. Inf. Retrieval (SIGIR’18)*, Ann Arbor, MI, Jul. 2018, pp. 515–524.
- [3] J. Han, L. Zheng, Y. Xu, B. Zhang, F. Zhuang, S. Y. Philip, and W. Zuo, “Adaptive deep modeling of users and items using side information for recommendation,” *IEEE Trans. Neural Netw. Learn. Syst.*, vol. 31, no. 3, pp. 737–748, Mar. 2020.
- [4] M. Gori, A. Pucci, V. Roma, and I. Siena, “ItemRank: A random-walk based scoring algorithm for recommender engines,” in *Proc. 20th Int. Joint Conf. Artif. Intell. (IJCAI’07)*, Hyderabad, India, Jan. 2007, pp. 2766–2771.
- [5] J.-H. Yang, C.-M. Chen, C.-J. Wang, and M.-F. Tsai, “HOP-rec: High-order proximity for implicit recommendation,” in *Proc. 12th ACM Conf. Recommender Syst. (RecSys’18)*, Vancouver, Canada, Oct. 2018, pp. 140–144.
- [6] M. Gao, L. Chen, X. He, and A. Zhou, “BiNE: Bipartite network embedding,” in *Proc. 41st Int. ACM SIGIR Conf. Res. Develop. Inf. Retrieval (SIGIR’18)*, Ann Arbor, MI, Jul. 2018, pp. 715–724.
- [7] C.-M. Chen, C.-J. Wang, M.-F. Tsai, and Y.-H. Yang, “Collaborative similarity embedding for recommender systems,” in *Proc. 28th Int. Conf. World Wide Web (WWW’19)*, San Francisco, CA, May 2019, pp. 2637–2643.
- [8] T. N. Kipf and M. Welling, “Semi-supervised classification with graph convolutional networks,” in *Proc. 5th Int. Conf. Learn. Representations (ICLR’17)*, Toulon, France, Apr. 2017.
- [9] W. Hamilton, Z. Ying, and J. Leskovec, “Inductive representation learning on large graphs,” in *Proc. 28th Int. Conf. Neural Inf. Process. Syst. (NIPS’17)*, Long Beach, CA, Dec. 2017, pp. 1025–1035.
- [10] K. Xu, W. Hu, J. Leskovec, and S. Jegelka, “How powerful are graph neural networks?” in *Proc. 7th Int. Conf. Learn. Representations. (ICLR’19)*, New Orleans, LA, May 2019.
- [11] P. Velickovic, G. Cucurull, A. Casanova, A. Romero, P. Liò, and Y. Bengio, “Graph attention networks,” in *Proc. 6th Int. Conf. Learn. Representations. (ICLR’18)*, Vancouver, Canada, Apr.–May 2018.
- [12] Z. Wu, S. Pan, F. Chen, G. Long, C. Zhang, and P. S. Yu, “A comprehensive survey on graph neural networks,” *IEEE Trans. Neural Netw. Learn. Syst.*, vol. 32, no. 1, pp. 4–24, Jan. 2021.
- [13] R. Ying, R. He, K. Chen, P. Eksombatchai, W. L. Hamilton, and J. Leskovec, “Graph convolutional neural networks for web-scale recommender systems,” in *Proc. 24th ACM SIGKDD Int. Conf. Knowl. Discovery and Data Mining (KDD’18)*, London, UK, Aug. 2018, pp. 974–983.
- [14] L. Zheng, C.-T. Lu, F. Jiang, J. Zhang, and P. S. Yu, “Spectral collaborative filtering,” in *Proc. 12th ACM Conf. Recommender Syst. (RecSys’18)*, Vancouver, Canada, Oct. 2018, pp. 311–319.

- [15] X. Wang, X. He, M. Wang, F. Feng, and T.-S. Chua, "Neural graph collaborative filtering," in *Proc. 42nd Int. ACM SIGIR Conf. Res. Develop. Inf. Retrieval (SIGIR'19)*, Paris, France, Jul. 2019, pp. 165–174.
- [16] X. Wang, R. Wang, C. Shi, G. Song, and Q. Li, "Multi-component graph convolutional collaborative filtering," in *Proc. 34th AAAI Conf. Artif. Intell. (AAAI'20)*, New York, NY, Feb. 2020, pp. 6267–6274.
- [17] L. Wu, Y. Yang, K. Zhang, R. Hong, Y. Fu, and M. Wang, "Joint item recommendation and attribute inference: An adaptive graph convolutional network approach," in *Proc. 43rd Int. ACM SIGIR Conf. Res. Develop. Inf. Retrieval (SIGIR'20)*, Virtual Event, China, Jul. 2020, pp. 679–688.
- [18] L. Chen, L. Wu, R. Hong, K. Zhang, and M. Wang, "Revisiting graph based collaborative filtering: A linear residual graph convolutional network approach," in *Proc. 34th AAAI Conf. Artif. Intell. (AAAI'20)*, New York, NY, Feb. 2020, pp. 27–34.
- [19] X. He, K. Deng, X. Wang, Y. Li, Y. Zhang, and M. Wang, "LightGCN: Simplifying and powering graph convolution network for recommendation," in *Proc. 43rd Int. ACM SIGIR Conf. Res. Develop. Inf. Retrieval (SIGIR'20)*, Virtual Event, China, Jul. 2020, pp. 639–648.
- [20] J. Zhu, Y. Yan, L. Zhao, M. Heimann, L. Akoglu, and D. Koutra, "Beyond homophily in graph neural networks: Current limitations and effective designs," in *Proc. 34th Int. Conf. Neural Inf. Process. Syst. (NIPS'20)*, Virtual Event, Dec. 2020, pp. 7793–7804.
- [21] H. Pei, B. Wei, K. C.-C. Chang, Y. Lei, and B. Yang, "Geom-GCN: Geometric graph convolutional networks," in *Proc. 8th Int. Conf. Learn. Representations (ICLR'20)*, Virtual Event, Apr. 2020.
- [22] J. Zhu, R. A. Rossi, A. Rao, T. Mai, N. Lipka, N. K. Ahmed, and D. Koutra, "Graph neural networks with heterophily," in *Proc. 35th AAAI Conf. Artif. Intell. (AAAI'21)*, Virtual Event, Feb. 2021, pp. 11168–11176.
- [23] T. Derr, Y. Ma, and J. Tang, "Signed graph convolutional networks," in *Proc. 18th IEEE Int. Conf. Data Mining (ICDM'18)*, Singap., Nov. 2018, pp. 929–934.
- [24] J. Huang, H. Shen, L. Hou, and X. Cheng, "Signed graph attention networks," in *Proc. 28th Int. Conf. Artif. Neural Netw. (ICANN'19)*, Munich, Germany, Sep. 2019, pp. 566–577.
- [25] F. Heider, "Attitudes and cognitive organization," *J. psychol.*, vol. 21, no. 1, pp. 107–112, 1946.
- [26] S. Rendle, C. Freudenthaler, Z. Gantner, and L. Schmidt-Thieme, "BPR: Bayesian personalized ranking from implicit feedback," in *Proc. 25th Conf. Uncertainty Artif. Intell. (UAI'09)*, Montreal, Canada, Jun. 2009, pp. 452–461.
- [27] Y. Koren, "Factorization meets the neighborhood: A multifaceted collaborative filtering model," in *Proc. 14th ACM SIGKDD Int. Conf. Knowl. Discovery and Data Mining (KDD'08)*, Las Vegas, NV, Aug. 2008, pp. 426–434.
- [28] Y. Koren, R. Bell, and C. Volinsky, "Matrix factorization techniques for recommender systems," *IEEE Computer*, vol. 42, no. 8, pp. 30–37, 2009.
- [29] X. Luo, M. Zhou, S. Li, Z. You, Y. Xia, and Q. Zhu, "A nonnegative latent factor model for large-scale sparse matrices in recommender systems via alternating direction method," *IEEE Trans. Neural Netw. Learn. Syst.*, vol. 27, no. 3, pp. 579–592, 2016.
- [30] C.-J. Lin, "Projected gradient methods for nonnegative matrix factorization," *Neural Comput.*, vol. 19, no. 10, pp. 2756–2779, 2007.
- [31] H. Xue, X. Dai, J. Zhang, S. Huang, and J. Chen, "Deep matrix factorization models for recommender systems," in *Proc. 26th Int. Joint Conf. Artif. Intell. (IJCAI'17)*, Melbourne, Aust., Aug. 2017, pp. 3203–3209.
- [32] X. He, L. Liao, H. Zhang, L. Nie, X. Hu, and T. Chua, "Neural collaborative filtering," in *Proc. 26th Int. Conf. World Wide Web (WWW'17)*, Perth, Aust., Apr. 2017, pp. 173–182.
- [33] X. Ning and G. Karypis, "SLIM: Sparse linear methods for top-N recommender systems," in *Proc. 11th IEEE Int. Conf. Data Mining (ICDM'11)*, Vancouver, Canada, Dec. 2011, pp. 497–506.
- [34] S. Kabbur, X. Ning, and G. Karypis, "FISM: Factored item similarity models for top-N recommender systems," in *Proc. 19th ACM SIGKDD Int. Conf. Knowl. Discovery and Data Mining (KDD'13)*. Chicago, IL: ACM, Aug. 2013, p. 659–667.
- [35] T. Nguyen and A. Takasu, "NPE: Neural personalized embedding for collaborative filtering," in *Proc. 27th Int. Joint Conf. Artif. Intell. (IJCAI'18)*, Stockholm, Sweden, Jul. 2018, pp. 1583–1589.
- [36] X. He, Z. He, J. Song, Z. Liu, Y.-G. Jiang, and T.-S. Chua, "NAIS: Neural attentive item similarity model for recommendation," *IEEE Trans. Knowl. Data Eng.*, vol. 30, no. 12, pp. 2354–2366, Dec. 2018.
- [37] S. Deng, L. Huang, G. Xu, X. Wu, and Z. Wu, "On deep learning for trust-aware recommendations in social networks," *IEEE Trans. Neural Netw. Learn. Syst.*, vol. 28, no. 5, pp. 1164–1177, 2017.
- [38] R. van den Berg, T. N. Kipf, and M. Welling, "Graph convolutional matrix completion," in *Proc. KDD'18 Deep Learning Day*, 2018.
- [39] M. Zhang and Y. Chen, "Inductive matrix completion based on graph neural networks," in *Proc. 8th Int. Conf. Learn. Representations (ICLR'20)*, Virtual Event, Apr. 2020.
- [40] L. Wu, P. Sun, Y. Fu, R. Hong, X. Wang, and M. Wang, "A neural influence diffusion model for social recommendation," in *Proc. 42nd Int. ACM SIGIR Conf. Res. Develop. Inf. Retrieval (SIGIR'19)*, Paris, France, Jul. 2019, pp. 235–244.
- [41] W. Fan, Y. Ma, Q. Li, Y. He, E. Zhao, J. Tang, and D. Yin, "Graph neural networks for social recommendation," in *Proc. 28th Int. Conf. World Wide Web (WWW'19)*, San Francisco, CA, May 2019, pp. 417–426.
- [42] L. Wu, J. Li, P. Sun, R. Hong, Y. Ge, and M. Wang, "DiffNet++: A neural influence and interest diffusion network for social recommendation," *IEEE Trans. Knowl. and Data Eng.*, to appear.
- [43] J. Kim, H. Park, J.-E. Lee, and U. Kang, "SIDE: Representation learning in signed directed networks," in *Proc. 27th Int. Conf. World Wide Web (WWW'18)*, Lyon, France, Apr. 2018, pp. 509–518.
- [44] W. Jin, T. Derr, Y. Wang, Y. Ma, Z. Liu, and J. Tang, "Node similarity preserving graph convolutional networks," in *Proc. 14th ACM Int. Conf. Web Search and Data Mining (WSDM'21)*, Virtual Event, Isr., Mar. 2021, pp. 148–156.
- [45] A. Vaswani, N. Shazeer, N. Parmar, J. Uszkoreit, L. Jones, A. N. Gomez, L. Kaiser, and I. Polosukhin, "Attention is all you need," in *Proc. 31st Int. Conf. Neural Inf. Process. Syst. (NIPS'17)*, Long Beach, CA, Dec. 2017, pp. 5998–6008.
- [46] J. Gilmer, S. S. Schoenholz, P. F. Riley, O. Vinyals, and G. E. Dahl, "Neural message passing for quantum chemistry," in *Proc. 34th Int. Conf. Mach. Learn. (ICML'17)*, Sydney, Aust., Aug. 2017, pp. 1263–1272.
- [47] K. Xu, C. Li, Y. Tian, T. Sonobe, K. Kawarabayashi, and S. Jegelka, "Representation learning on graphs with jumping knowledge networks," in *Proc. 35th Int. Conf. Mach. Learn. (ICML'18)*, Stockholm, Sweden, Jul. 2018, pp. 5449–5458.
- [48] Q. Li, Z. Han, and X.-M. Wu, "Deeper insights into graph convolutional networks for semi-supervised learning," in *Proc. 32nd AAAI Conf. Artif. Intell. (AAAI'18)*, New Orleans, LA, Feb. 2018, pp. 3538–3545.
- [49] T. Mikolov, I. Sutskever, K. Chen, G. S. Corrado, and J. Dean, "Distributed representations of words and phrases and their compositionality," in *Proc. 27th Conf. Neural Inf. Process. Systems (NIPS'13)*, Lake Tahoe, NV, Dec. 2013, pp. 3111–3119.
- [50] J. Tang, M. Qu, M. Wang, M. Zhang, J. Yan, and Q. Mei, "LINE: Large-scale information network embedding," in *Proc. 24th Int. Conf. World Wide Web (WWW'15)*, Florence, Italy, May 2015, pp. 1067–1077.
- [51] F. M. Harper and J. A. Konstan, "The movielens datasets: History and context," *ACM Trans. Interactive Intell. Syst.*, vol. 5, no. 4, pp. 1–19, Dec. 2015.
- [52] R. He and J. McAuley, "Ups and downs: Modeling the visual evolution of fashion trends with one-class collaborative filtering," in *Proc. 25th Int. Conf. World Wide Web (WWW'16)*, Montreal, Canada, Apr. 2016, pp. 507–517.
- [53] —, "VBPR: Visual bayesian personalized ranking from implicit feedback," in *Proc. 30th AAAI Conf. Artif. Intell. (AAAI'16)*, Phoenix, AZ, Feb. 2016, pp. 144–150.
- [54] K. Järvelin and J. Kekäläinen, "Cumulated gain-based evaluation of IR techniques," *ACM Trans. Inf. Syst.*, vol. 20, no. 4, pp. 422–446, Oct. 2002.
- [55] M. Fey and J. E. Lenssen, "Fast graph representation learning with pytorch geometric," in *Proc. ICLR Workshop on Representation Learning on Graphs and Manifolds*, New Orleans, LA, May 2019.
- [56] X. Glorot and Y. Bengio, "Understanding the difficulty of training deep feedforward neural networks," in *Proc. 13th Int. Conf. Artif. Intell. Statist. (AISTATS'10)*, Sardinia, Italy, May 2010, pp. 249–256.
- [57] N. Srivastava, G. Hinton, A. Krizhevsky, I. Sutskever, and R. Salakhutdinov, "Dropout: A simple way to prevent neural networks from overfitting," *J. Mach. Learn. Res.*, vol. 15, no. 1, pp. 1929–1958, Jan. 2014.
- [58] D. P. Kingma and J. Ba, "Adam: A method for stochastic optimization," in *Proc. 3rd Int. Conf. Learn. Representations (ICLR'15)*, San Diego, CA, May 2015.